Anisotropic diffusion of nbutane on a stepped Ru(001) surface

M. V. Arena, E. D. Westre, and S. M. George

Citation: The Journal of Chemical Physics **96**, 808 (1992); doi: 10.1063/1.462466
View online: http://dx.doi.org/10.1063/1.462466
View Table of Contents: http://scitation.aip.org/content/aip/journal/jcp/96/1?ver=pdfcov
Published by the AIP Publishing

Anisotropic diffusion of *n*-butane on a stepped Ru(001) surface

M. V. Arena, E. D. Westre, and S. M. George
Department of Chemistry, Stanford University, Stanford, California 94305-5080

(Received 14 August 1991; accepted 20 September 1991)

The surface diffusion of *n*-butane on a stepped ruthenium {Ru(*S*)-[15(001)×2(100)]} surface was studied using laser-induced thermal desorption (LITD) techniques. Large aspect ratio laser desorption areas were used to measure the anisotropy of *n*-butane diffusion on the stepped Ru(001) surface. Surface diffusion coefficients at $\Theta = \Theta_{sat}$ for diffusion parallel ($D_{\parallel}$) or perpendicular ($D_{\perp}$) to the steps were measured by orienting these desorption areas either perpendicular or parallel to the step edges. At 115 K, the surface diffusion coefficient was much larger in the direction parallel to the step edges and $D_{\parallel}/D_{\perp} \approx 26$. Surface diffusion coefficients for diffusion on a terrace (D_t) or over a step (D_s) were deconvoluted from the measured $D_{\parallel}$ and $D_{\perp}$ values. The temperature-dependent $D_{\parallel}$ and $D_{\perp}$ values yielded an activation barrier for *n*-butane diffusion on the Ru(001) terrace at $\Theta = \Theta_{sat}$ of $E_t = 2.8 \pm 0.4$ kcal/mol and a diffusion preexponential of $D_{0,t} = 1.6 \times 10^{-2 \pm 0.2}$ cm^2/s. For diffusion over a step at $\Theta = \Theta_{sat}$, the surface diffusion barrier was $E_s = 4.8 \pm 0.5$ kcal/mol and the diffusion preexponential was $D_{0,s} = 6.1 \times 10^{-1 \pm 0.3}$ cm^2/s. The measured corrugation ratio for *n*-butane on the Ru(*S*)-[15(001)×2(100)] surface was $\Omega \equiv E_{dif}/E_{des} = 0.24$ for diffusion on the terrace and $\Omega = 0.41$ for diffusion over a step. The surface corrugation ratio on the terrace of Ru(*S*)-[15(001)×2(100)] was similar to $\Omega = 0.29$ measured previously for *n*-butane on Ru(001). This similarity indicated that step defects did not dominate previous LITD measurements of alkanes on Ru(001).

I. INTRODUCTION

The effect of steps on surface diffusion is an important issue in surface kinetics.[1] Surface steps will modulate the surface potential and alter surface structure and adsorbate binding. Steps could act as traps or blocks depending on the details of the surface potential. Despite the significance of surface steps in the kinetics of heterogeneous catalysis, very few surface mobility studies have been performed.[2-11] This study will focus on the effect of steps on the diffusion of a model alkane on Ru(001).

The surface diffusion of physisorbed alkanes on Ru(001) has been examined recently with laser-induced thermal desorption (LITD) techniques.[12-17] Measurements for *n*-alkanes,[12] cycloalkanes,[13] and branched alkanes[14] have examined the effect of molecular structure and composition on alkane surface mobility. These studies measured the diffusion and desorption activation barriers E_{dif} and E_{des}, and reached the conclusion that the surface corrugation ratio was constant at $\Omega \equiv E_{dif}/E_{des} \approx 0.3$. This constant corrugation ratio for every alkane argued for a similar binding configuration and concerted motion mechanism for all the alkanes.[12-17]

This current study continued to explore alkane surface diffusion and examined the influence of steps on *n*-butane surface diffusion on Ru(001). In a previous article, the coverage dependence of *n*-butane diffusion was examined on a stepped Ru surface Ru(*S*)-[15(001)×2(100)].[18] The surface diffusion coefficient was strongly coverage dependent and increased by four orders of magnitude as the coverage increased from $\Theta = 0.05\Theta_{sat}$ to $\Theta = \Theta_{sat}$. This coverage dependence was consistent with the trapping of *n*-butane molecules at step sites. Once the step sites were saturated, *n*-butane was observed to move nearly unimpeded across the Ru(001) terraces.

This work will complement the previous study by examining the anisotropy of *n*-butane surface diffusion on Ru(*S*)-[15(001)×2(100)]. In general, the surface diffusion coefficient is a second-order tensor.[19] Fick's second law in tensor notation is given below

$$\frac{\partial \Theta}{\partial t} = \begin{pmatrix} D_{xx} & D_{xy} \\ D_{yx} & D_{yy} \end{pmatrix} \nabla^2 \Theta. \tag{1}$$

A transformation may be found to diagonalize the diffusion tensor

$$D = \begin{pmatrix} D_{aa} & 0 \\ 0 & D_{bb} \end{pmatrix}, \tag{2}$$

where **a** and **b** are the principal axes. For a stepped surface, the principal axes are simply the directions perpendicular and parallel to the step edges and the tensor components D_{aa} and D_{bb} become $D_{\parallel}$ and $D_{\perp}$. In this study, the $D_{\parallel}$ and $D_{\perp}$ tensor components were measured for the first time on stepped surfaces using LITD techniques.

This study will reveal clearly the effects of steps on *n*-butane surface diffusion on Ru(001). A criticism of surface diffusion measurements by the LITD method is that these macroscopic measurements might be dominated by surface steps or defects.[9,10,20] Although none of this criticism has been substantiated, the impression has been left that LITD techniques cannot obtain the kinetics that characterize mobility on single-crystal surfaces. This work will refute the earlier suggestions and demonstrate clearly the role of steps on LITD measurements of surface diffusion.

 0021-9606/92/010808-09$06.00

II. EXPERIMENT

An initial laser pulse is used to heat a well-defined area on the surface in the traditional LITD surface diffusion experiment.[21,22] The laser heating induces a rapid temperature jump that is sufficient to desorb the adsorbates within the heated area.[23,24] After a time delay, a second identical probe laser pulse heats the same area. Consequently, the adsorbates that have diffused into the initially evacuated region from the surrounding surface are desorbed from the surface.

A quadrupole mass spectrometer measures the desorption flux and the mass signal at each delay time corresponds to the amount of diffusional refilling. Subsequently, the time-dependent refilling signals are fit using the appropriate solution to Fick's second law to determine the surface diffusion coefficient. This prepare and probe experimental procedure has been employed successfully in many recent studies to measure surface diffusion on single-crystal metal surfaces.[12-17,21,22,25-36]

In order to measure anisotropic diffusion with the LITD method, a large aspect ratio desorption area is required.[37-39] Desorption areas used in previous LITD diffusion studies had an aspect ratio of 1.7. To obtain larger aspect ratio desorption areas, a series of overlapping desorption spots was created on the surface. Each desorption area consisted of 21 overlapping spots as shown schematically in Fig. 1. The aspect ratio for the horizontal desorption area was 18.7 to 1. The aspect ratio for the vertical desorption area was 6.6 to 1.

The refilling signal for these large aspect ratio desorption areas will be dominated by diffusion in the direction parallel to the short axis of the desorption area. The crystal was oriented so that the step edges were parallel to the horizontal direction. For a desorption area oriented vertically, the refilling will be dominated by diffusion parallel to the step edges. Likewise, a desorption area oriented horizontally will have its refilling dominated by diffusion perpendicular to the step edges.

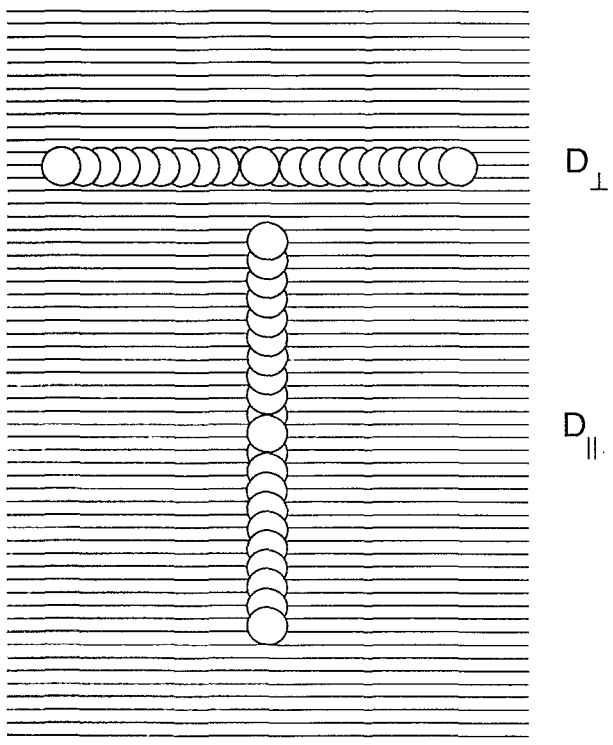

FIG. 1. A depiction of the overlapping laser desorption spots comprising the large aspect ratio desorption areas used for the LITD measurements of diffusion anisotropy. The horizontal lines represent the step edges.

The experimental setup for LITD surface diffusion measurements has been described previously.[21] The experiments were performed in an ion-pumped UHV chamber that maintained background pressures below 3×10^{-10} Torr. The characterization of surface cleanliness and surface order was performed with Auger electron spectroscopy (AES) using a single-pass cylindrical mirror analyzer (CMA) and low energy electron diffraction (LEED) spectrometry.

These LITD experiments utilized a TEM-00 *Q*-switched Nd:phosphate glass laser producing pulse lengths of 100–130 ns with Gaussian spatial profiles. Longer *Q*-switched laser pulse lengths significantly reduce the risk of surface damage during laser heating.[40] In the present study, the laser pulse energy before entering the UHV chamber was 0.15 mJ/pulse. The pulses were focused by a 65 cm focal length lens to give a Gaussian spatial profile of 120 μm [full-width at half-maximum (FWHM)] at the focus of the lens.

The stepped surface was positioned at the focus of the lens and the angle between the incoming laser pulses and the surface normal was 54°. Each individual desorption spot was elliptical with an aspect ratio of 1.7. The dimensions of a single desorption spot were approximately 100 μm in diameter along the minor axis and 170 μm in diameter along the major axis.[22] The major axis of these low aspect ratio desorption areas was aligned parallel to the step edges on the stepped Ru(001) surface.

The *n*-butane was adsorbed onto the Ru(001) stepped surface using a glass capillary array doser. The doser was positioned $\approx$2 cm from the Ru(001) stepped surface. The doser produced consistent coverages as determined by temperature-programmed desorption (TPD) analysis. All diffusion experiments were performed at $\Theta = \Theta_{sat}$. Using LITD spatial measurements, the coverage of *n*-butane on the stepped surface was found to be uniform to within $\pm$7% across the surface.

The surface cleaning procedure has been discussed earlier.[30-36] The cleaning procedure was conducted after each experiment and the surface cleanliness was monitored using both CO TPD peak temperatures and AES as discussed previously.[35,36] The Ru(001) stepped surface was biased to $-$80 V to repel any stray electrons for all the LITD and TPD experiments.[41]

For each surface diffusion experiment, the Ru(001) stepped surface was cleaned, dosed at a lower temperature, and subsequently heated to the desired experimental temperature. The high aspect ratio desorption areas were produced by translating the laser beam across the Ru(001) stepped surface. This translation was accomplished using mirrors mounted on piezoelectric translators with optical encoders. The desorption areas were always separated by at least 700 μm.

To ensure complete evacuation of the central desorption

area, each center desorption spot was prepared with five consecutive laser pulses.[40] The other desorption spots that defined the high aspect ratio desorption area were prepared with two desorption laser pulses. Each of the central desorption spots was probed with a second sequence of nearly identical laser pulses at time delays ranging from 6 to 1800 s. The piezoelectric translators returned the laser to each of the desorption spots with an accuracy of ± 0.5 μm. Control experiments indicated that adsorption from the background pressure in the UHV chamber was insignificant.

The stepped crystal utilized for these experiments was obtained from Bud Addis at the crystal shop in the Department of Materials Science and Engineering at Cornell University. The stepped Ru(001) surface was prepared by cutting at an angle of 7.2° to the (001) surface plane along the $(1,0,\bar{1},0)$ direction. Back-reflection Laué x-ray analysis confirmed the cut angle and direction after polishing the crystal optically flat. This plane should result in a $(1,0,\bar{1},15)$ surface that has (001) terraces and (100) step faces.

The LEED pattern observed for the stepped Ru(001) surface indicated that the average terrace had a length of 15 atomic rows.[18] Additional LEED studies of the (0,0) spot splitting were performed vs incident electron energy.[42,43] These measurements yielded a step height of 4.1 ± 0.5 Å which is approximately two atomic layers.[18] A step of two atomic layers is consistent with the cut angle and terrace length. This crystal surface would be designated Ru(*S*)-[15(001)×2(100)] in terrace-step notation.[18,44] This surface is shown schematically in Fig. 2. Double atomic steps on metals have been observed on both platinum[45] and ruthenium[46] stepped surfaces. In particular, a double atomic step on Ru(001) of 4.28 Å was previously deduced based on LEED measurements.[46]

III. RESULTS

A. Anisotropy

The analysis of refilling curves for high aspect ratio desorption areas is more complex than typical LITD diffusional refilling curves. Initially, the experimental refilling curves were fit with predicted refilling curves derived from Fick's second law assuming isotropic diffusion. The predicted curves were based on a constant surface diffusion coefficient and were generated using the point-source method.[47] After an estimate of the diffusion anisotropy was obtained, the experimental refilling curves were refit to new predicted curves that accounted for anisotropic diffusion. Again, the point-source method was used to generate these new curves.[47] This procedure was repeated until the experimental results and the predictions were self-consistent.

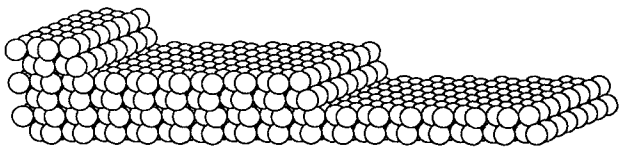

FIG. 2. A representation of the stepped Ru(001) surface as determined by LEED and Laué x-ray diffraction studies. This surface is designated as Ru(*S*)-[15(001)×2(100)] in step-terrace notation.

The surface diffusion coefficient for *n*-butane on Ru(*S*)-[15(001)×2(100)] was strongly coverage dependent due to trapping at the steps.[18] Fitting the experimental refilling curves with a constant surface diffusion coefficient at long delay times provides an estimate for the actual surface diffusion coefficient. Earlier simulations have shown that these fits provide an accurate estimate of the diffusion coefficient.[48] In addition, simulations based on the measured coverage dependence indicate that this estimate is very accurate at $\Theta = \Theta_{sat}$, where the estimated diffusion coefficient is approximately 20% lower than the actual diffusion coefficient.[18] This small error is well within the typical scatter for individual experiments. As mentioned earlier, all experiments were conducted at $\Theta = \Theta_{sat}$.

Figure 3 shows normalized refilling data at $\Theta = \Theta_{sat}$ for *n*-butane diffusion on Ru(*S*)-[15(001)×2(100)] at 115 K. Refilling curves are shown for diffusion perpendicular and parallel to the step edges. The high aspect ratio laser desorption areas oriented in the horizontal direction parallel to the step edges had diameters of 120 μm along the minor axis and 2240 μm along the major axis. Similarly, the high aspect ratio laser desorption areas oriented in the vertical direction perpendicular to the step edges had diameters of 200 μm along the minor axis and 1320 μm along the major axis.

The surface diffusion coefficient was larger by a factor of ≈ 26 for diffusion in the direction parallel to the step edges. The surface diffusion coefficient for diffusion parallel to the

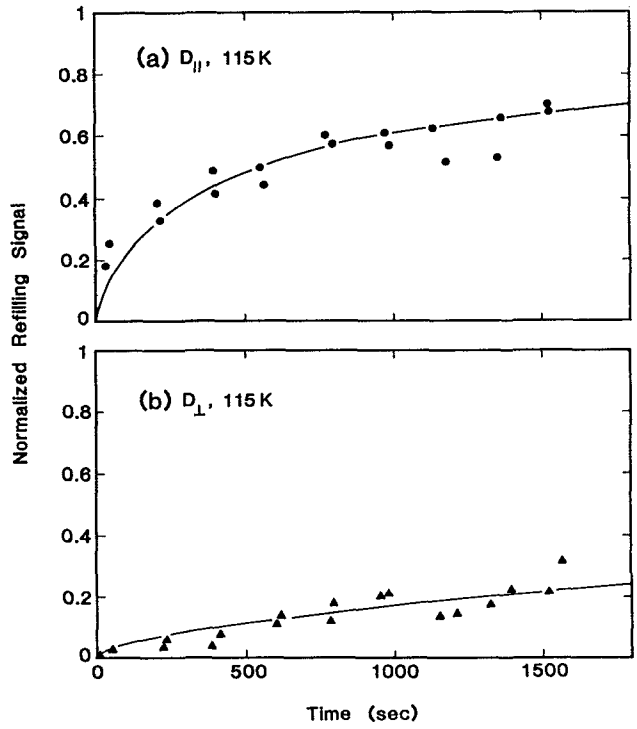

FIG. 3. Anisotropic diffusional refilling data at 115 K for *n*-butane at $\Theta = \Theta_{sat}$ on Ru(*S*)-[15(001)×2(100)]. The refilling curve for diffusion parallel to the step edges corresponds to $D_{\parallel} = 1.0 \times 10^{-7}$ cm^2/s. The refilling curve for diffusion perpendicular to the step edges corresponds to $D_{\perp} = 3.9 \times 10^{-9}$ cm^2/s. Solid lines represent refilling curves corresponding to constant surface diffusion coefficients.

step edges at 115 K was $D_{\parallel} = 1.0\times10^{-7}$ cm^2/s. The surface diffusion coefficient for diffusion perpendicular to the step edges at 115 K was $D_{\perp} = 3.9\times10^{-9}$ cm^2/s.

Surface diffusion may also be anisotropic in the direction perpendicular to the step edges.[49] For example, diffusion might be slower in a direction going up the steps than down the steps. To check for this additional anisotropy, a rectangular desorption area was created on the surface using overlapping laser shots. The desorption area had dimensions of about 1200 μm in width and 480 μm in height. Refilling signals were probed at both the top and bottom edges of the rectangle. Within the scatter of the desorption signals, no difference could be observed between refilling signals in the direction either up or down a step edge at $\Theta = \Theta_{sat}$.

B. Temperature dependence

The normalized refilling data vs temperature for *n*-butane on Ru(*S*)-[15(001)×2(100)] at $\Theta = \Theta_{sat}$ is displayed in Fig. 4. The dimensions of the laser desorption areas for these experiments were approximately 130×2430 μm for the horizontal desorption area and 220×1430 μm for the vertical desorption area. Refilling curves are shown for diffusion parallel and perpendicular to the steps. As expected for a thermally activated diffusion mechanism, the diffusional refilling was faster at higher temperatures. The solid lines show fits to these refilling curves derived from Fick's second law. These fits assumed a constant diffusion coefficient.

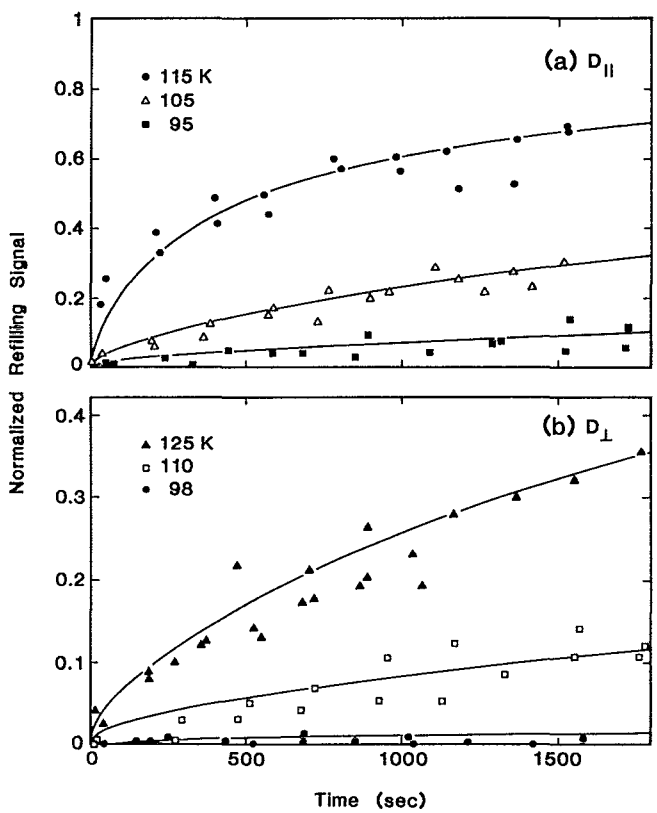

FIG. 4. Anisotropic diffusional refilling data for *n*-butane at $\Theta = \Theta_{sat}$ on Ru(*S*)-[15(001)×2(100)] at various temperatures. (a) Refilling curves for diffusion parallel to the step edges. (b) Refilling curves for diffusion perpendicular to the step edges. Solid lines represent refilling curves corresponding to constant surface diffusion coefficients.

C. Surface decomposition

The possible surface decomposition for *n*-butane on Ru(*S*)-[15(001)×2(100)] was determined by measuring the carbon remaining after the *n*-butane had thermally desorbed. The amount of carbon on the surface was measured by monitoring the peak-to-peak height ratio of the Ru 273 eV AES signal to the Ru 231 eV AES signal.[30,50] No surface carbon could be observed after any of the diffusion experiments.

The decomposition kinetics and extent of surface decomposition can also be measured using LITD techniques.[51,52] For all coverages, no decrease in the *n*-butane LITD signals was observed after the diffusion experiments from 95 to 125 K. This steady LITD signal indicates that the surface coverage of *n*-butane was constant during the experiments. The surface coverage did not change even when all the *n*-butane was trapped at step edges at low coverages. There was no evidence for decomposition of *n*-butane on Ru(*S*)-[15(001)×2(100)] under the experimental conditions used for the surface diffusion experiments.

IV. DECONVOLUTION

The values $D_{\perp}$ and $D_{\parallel}$ are convolutions of D_t and D_s, where D_t is the surface diffusion coefficient over a flat terrace and D_s is the surface diffusion coefficient over an isolated step. Figure 5 shows a schematic representation of diffu-

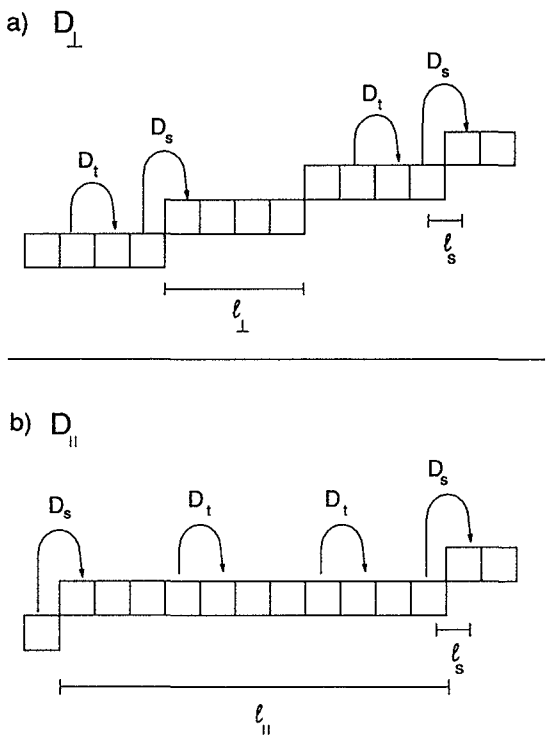

FIG. 5. A schematic representation of $D_{\perp}$ and $D_{\parallel}$ in terms of D_t, D_s, $l_{\perp}$, l_s, and $l_{\parallel}$.

sion in directions parallel and perpendicular to the step edges. The distance $l_\perp$ is the terrace length perpendicular to the step edges. The distance $l_\parallel$ is the terrace length parallel to the step edges. The value l_s is the jump distance between adjacent terraces.

The diffusion coefficient for $D_\perp$ will characterize the result of diffusing a distance of $l_\perp - l_s$ with a surface diffusion coefficient of D_t and a distance l_s with a surface diffusion coefficient of D_s. Likewise, the diffusion coefficient for $D_\parallel$ will represent the result of diffusing a distance $l_\parallel - l_s$ with a surface diffusion coefficient of D_t and a distance of l_s with a surface diffusion coefficient of D_s. Terraces with finite widths of $l_\parallel$ in the direction parallel to the step edges are included because no macroscopic single-crystal surface is free of step defects.

The method of deconvoluting the various surface diffusion coefficients is analogous to heterogeneous diffusion in laminates where there are different diffusion rates in the various layers.[19] For a laminate composed of n sheets placed in series, the relationship for the net diffusion coefficient is given by

$$\frac{l_{\text{tot}}}{D_{\text{nel}}} = \sum_{i=1}^{n} \frac{l_i}{D_i}, \tag{3}$$

where D_i is the diffusion coefficient and l_i is the length in the ith layer.

By making the analogy between surface distances and layer thicknesses, the relationship between D_t, D_s, $D_\perp$, l_s, and $l_\perp$ is given below

$$\frac{l_\perp}{D_\perp} = \frac{(l_\perp - l_s)}{D_t} + \frac{l_s}{D_s}. \tag{4}$$

A similar relation for D_t, D_s, $D_\parallel$, l_s, and $l_\parallel$ can also be obtained

$$\frac{l_\parallel}{D_\parallel} = \frac{(l_\parallel - l_s)}{D_t} + \frac{l_s}{D_s}. \tag{5}$$

By combining and rearranging Eqs. (4) and (5), values for D_t and D_s based on $D_\parallel$, $l_\parallel$, $D_\perp$, $l_\perp$, and l_s may be derived

$$D_s = \left\{ \frac{l_s(l_\parallel - l_\perp)}{l_\perp(l_\parallel - l_s)/D_\perp - (l_\perp - l_s)l_\parallel/D_\parallel} \right\}, \tag{6}$$

$$D_t = \left\{ \frac{l_\parallel - l_\perp}{l_\parallel/D_\parallel - l_\perp/D_\perp} \right\}. \tag{7}$$

Values for D_t and D_s may be determined from measurements of $D_\parallel$ and $D_\perp$ at the same temperature. A value of $l_\perp = 32.9$ Å can be determined from the terrace length of 15 atomic rows as measured by LEED. A value for $l_s = 4.7$ Å, i.e., two atomic rows, may also be estimated based on the schematic of the surface shown in Fig. 2. This value for l_s is the horizontal distance between the last row of metal atoms on the upper terrace and the first exposed row of metal atoms on the adjacent lower terrace.

A value for $l_\parallel$ is not as simple to ascertain. However, surface diffusion coefficients at low temperature resulting from Eqs. (6) and (7) will result in negative values if $l_\parallel$ is too small. Surface diffusion coefficients at low temperatures will also be faster than values at higher temperature if $l_\parallel$ is too small. Such values would not be physically realistic. Consequently, the value of $l_\parallel$ was fit so that surface diffusion coefficients were obtained that were nonnegative and did not increase at lower temperatures.

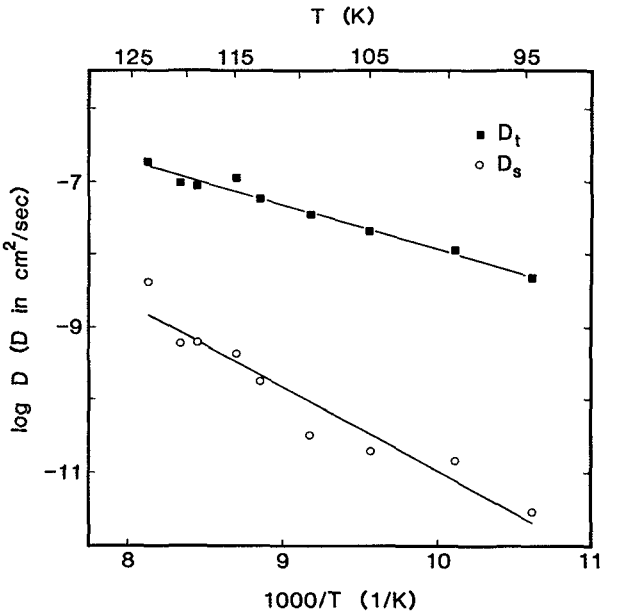

FIG. 6. An Arrhenius plot of the surface diffusion coefficients for *n*-butane at $\Theta = \Theta_{\text{sat}}$ on a terrace and over a step on Ru(*S*)-[15(001)×2(100)]. The measured surface diffusion kinetic parameters on a terrace were $E_t = 2.8 \pm 0.4$ kcal/mol and $D_{0,t} = 1.6\times10^{-2\pm0.2}$ cm²/s. The measured surface diffusion kinetic parameters over a step were $E_s = 4.8 \pm 0.5$ kcal/mol and $D_{0,s} = 6.1\times10^{-1\pm0.3}$ cm²/s.

The surface diffusion activation barriers E_s and E_t and the surface diffusion preexponentials $D_{0,s}$ and $D_{0,t}$ may be determined from an Arrhenius analysis by plotting $\ln(D)$ vs $1/T$. The Arrhenius plots for the surface diffusion of *n*-butane at $\Theta = \Theta_{\text{sat}}$ over a terrace and step on Ru(*S*)-[15(001)×2(100)] are shown in Fig. 6. The data points represent averages of one to four experiments.

The surface diffusion barrier is $E_t = 2.8 \pm 0.4$ kcal/mol and the diffusion preexponential is $D_{0,t} = 1.6\times10^{-2\pm0.2}$ cm²/s for diffusion over a terrace. Similarly, the surface diffusion barrier is $E_s = 4.8 \pm 0.5$ kcal/mol and the diffusion preexponential is $D_{0,s} = 6.1\times10^{-1\pm0.3}$ cm²/s for diffusion over a step. Uncertainties were based on the standard deviation of the slope and y intercept using standard error propagation methods. Based on the criteria discussed above, the value for $l_\parallel$ was estimated to be 6000 Å.

V. DISCUSSION

A. Anisotropy

The surface diffusion of *n*-butane on Ru(*S*)-[15(001)×2(100)] was anisotropic. At 115 K, diffusion parallel to the step edges was significantly faster than diffusion perpendicular to the step edges and $D_\parallel/D_\perp \approx 26$. In addition, the surface diffusion coefficient observed for mobility parallel to the step edges was similar to the surface mobility for *n*-butane measured on Ru(001).[12]

Figure 7 shows a predicted surface potential for *n*-butane on Ru(*S*)-[15(001)×2(100)].[18] The potential shows

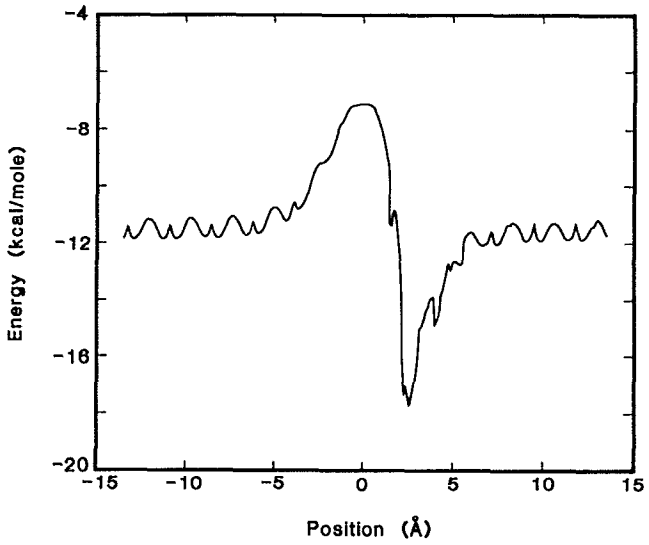

FIG. 7. The calculated surface potential for *n*-butane on Ru(*S*)-[15(001)×2(100)] for molecular motion perpendicular to a step edge. The origin represents the center of the last row of Ru atoms on the upper terrace.

the change in binding energy for movement perpendicular to the step. For these calculations, the orientation of the *n*-butane molecule was approximately parallel to the step edge. Figure 7 was generated by summing Lennard-Jones (6-12) pair interactions between the atoms in the *n*-butane molecule and the surface Ru atoms on Ru(*S*)-[15(001)×2(100)]. This approach has been described elsewhere.[53]

The predicted surface potential shows a strongly bound state for *n*-butane lying parallel at the step edge. The surface potential in Fig. 7 also shows a significantly higher barrier to diffusion over a step edge compared with diffusion on the terrace. For molecular motion down a step, the calculated surface diffusion barrier is approximately $E_s = 4.7$ kcal/mol. The calculated barrier for surface diffusion up a step edge is significantly higher at $E_s = 10.6$ kcal/mol. The surface potential shown in Fig. 7 is for an isolated *n*-butane molecule.

The $D_{\parallel}$ and $D_{\perp}$ surface diffusion coefficients measured for *n*-butane on Ru(*S*)-[15(001)×2(100)] were performed at $\Theta = \Theta_{sat}$. At this high coverage, the trap sites next to the step edges would very quickly become occupied by *n*-butane molecules. Therefore, an *n*-butane molecule that diffuses over a step may not be influenced by the trap site. Rather, the *n*-butane molecules that are trapped initially at the step edges may smooth out the surface potential. As a result, the barrier to diffusion over a step may be nearly equivalent in both directions. This proposed smoothing could be the reason why no anisotropy was observed for diffusion up or down the step edge.

The calculated value for the surface diffusion barrier over an isolated step is $E_s = 4.7$ kcal/mol. The calculated value is very close to the experimentally observed value of $E_s = 4.8 \pm 0.5$ kcal/mol. In contrast, there is not agreement between experiment and theory for the surface diffusion barriers on the terrace. The theoretical predictions for the diffusion activation energy on the terrace E_t are low by a factor of 3 compared with the measured activation barriers.[53]

The surface diffusion preexponentials $D_{0,t}$ and $D_{0,s}$ show a compensation with respect to the diffusion barrier. For diffusion over a step, the larger activation barrier E_s is accompanied by a larger preexponential of $D_{0,s} = 6.1 \times 10^{-1 \pm 0.3}$ cm^2/s. This larger value can be explained qualitatively using transition state theory.[54] For diffusion over a step and along a terrace, the initial states are nearly equivalent. However, the transition state for diffusion over a step is much higher in energy and farther away from the surface compared with the transition state for diffusion along the terrace. Consequently, the transition state for *n*-butane diffusing over a step would be more like a two-dimensional gas molecule and the preexponential would be expected to be much larger.

B. Limitations of the deconvolution analysis

1. Value of $l_{\parallel}$

The deconvolution results are dependent on the $l_{\parallel}$ value. Based on a typical miscut angle of 0.5°, a value for $l_{\parallel}$ would be estimated to be approximately 507 Å. In comparison, the value of $l_{\parallel} = 6000$ Å utilized in the analysis may seem unrealistically high. However, a miscut in the direction parallel to the steps may not result in as many steps as expected. Instead, the surface could kink along the step edge and unusually long terrace lengths would be measured in a direction parallel to the step edge. In addition, small random defects may not contribute to $l_{\parallel}$ because *n*-butane molecules may move easily around these sites once they have been titrated by other *n*-butane molecules.

Recent experiments have observed long atomically flat terraces on stepped surfaces. Scanning-tunneling-microscopy (STM) studies have observed atomically flat lengths on a Pd(100) surface of over 2000 Å in length.[55] Other STM studies have observed flat lengths greater than 1400 Å on Au(111),[56,57] 3000 Å on Au(110),[58] and 3000 Å on Pt(111).[59] The value for $l_{\parallel}$ is not unreasonable compared with the observed flat lengths listed above.

The self-consistency for $l_{\parallel}$ and the other kinetic parameters can be explored by comparing the observed data with predicted values for $D_{\perp}$ and $D_{\parallel}$ based on $l_{\perp}$, l_s, E_s, E_t, $D_{0,s}$ and $D_{0,t}$. Figure 8 shows the plot of the experimental data and the predicted trends vs temperature for both $D_{\parallel}$ and $D_{\perp}$. The trends based on E_s, E_t, $D_{0,s}$, and $D_{0,t}$ are slightly curved and hence not strictly Arrhenius. However, the predicted trends for $D_{\perp}$ and $D_{\parallel}$ are in good agreement with the observed values. The curvature becomes much more pronounced for values smaller than $l_{\parallel} = 6000$ Å.

Using the parameters E_s, E_t, $D_{0,s}$ and $D_{0,t}$ derived from the Ru(*S*)-[15(001)×2(100)] experiments, a value for the terrace length on the Ru(001) surface can be estimated using the previously measured surface diffusion barrier of $E_{dif} = 3.5$ kcal/mol on Ru(001).[12] Net surface diffusion coefficients were calculated at various temperatures based on a fixed terrace length l. Kinetic parameters for surface diffusion were derived by a standard Arrhenius analysis. A surface diffusion barrier of $E_{obs} = 3.5$ kcal/mol was determined

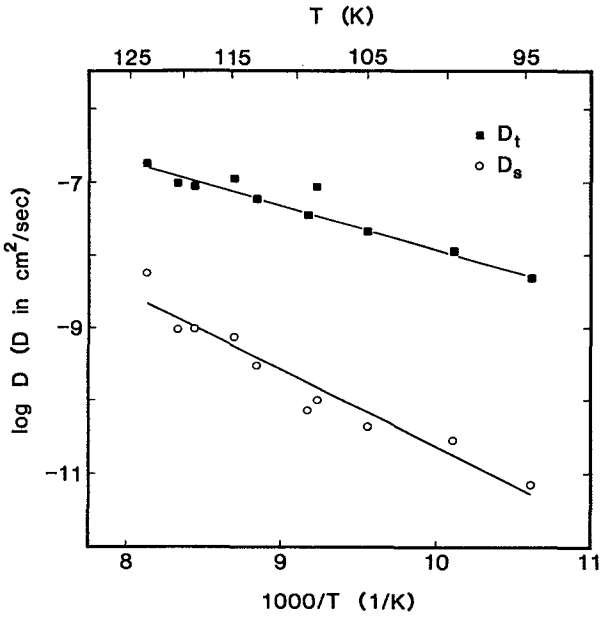

FIG. 8. Arrhenius plots of $D_{\parallel}$ and $D_{\perp}$ for *n*-butane at $\Theta = \Theta_s$ on Ru(*S*)-[15(001)×2(100)]. The solid lines are fits to the data based on the measured values for E_s, E_t, $D_{0,s}$, $D_{0,t}$, and $l_{\perp}$ with $l_{\parallel} = 6000$ Å and $l_s = 4.7$ Å.

for a terrace length of $l \approx 2500$ Å.

Figure 9 displays a plot of the surface diffusion barrier E_{dif} vs the logarithm of the terrace length l. This plot shows the effect of terrace length on the observed diffusion barrier. The parameters used for this figure were the E_s, E_t, $D_{0,s}$, and $D_{0,t}$ values obtained from the deconvolution analysis. In the limit where $l = 1$ Å, the surface diffusion barrier is $E_{\text{dif}} = E_s$. Similarly, the surface diffusion barrier is $E_{\text{dif}} \approx E_t$ when $l = 1\,000\,000$ Å. The surface diffusion barrier changes most rapidly between $l \approx 100$ and $l \approx 10\,000$ Å. This plot illustrates the effect of steps on the diffusion activation barrier measured by LITD techniques.

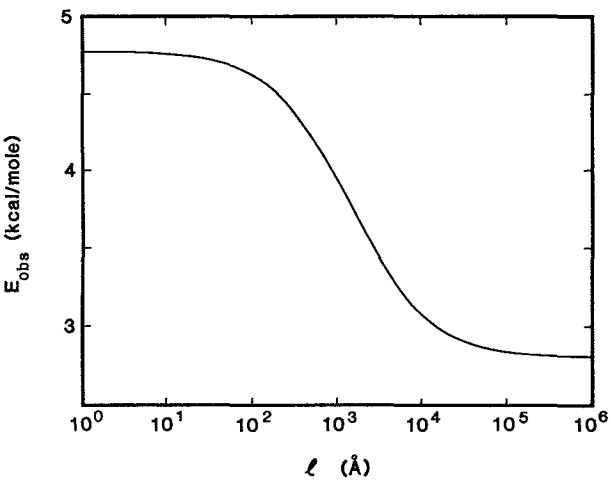

FIG. 9. Surface diffusion activation barrier that would be expected for *n*-butane diffusion on a stepped Ru(001) surface as a function of the terrace length.

2. Misalignment error

Exact alignment of the step edges of the crystal with the horizontal translation direction of the laser is difficult. However, the possible error in the measurement due to the misalignment can be estimated. For an experimentally observed diffusion coefficient D_{obs}, the relationship between $D_{\parallel}$ and $D_{\perp}$ is given by[19]

$$D_{\text{obs}} = D_{\parallel} \cos^2 \varphi + D_{\perp} \sin^2 \varphi. \tag{8}$$

In this expression, φ is the angle between the minor axis of the high aspect ratio desorption area and the step edges. $D_{\parallel}$ and $D_{\perp}$ are the true diffusion coefficients in the parallel and perpendicular directions, respectively.

Assuming a misalignment angle of $\varphi = 5°$, new values for E_t, E_s, $D_{0,t}$ and $D_{0,s}$ were calculated. This value for φ represents a worse case estimate. The kinetic parameters for surface diffusion over a terrace would become $E_t = 2.8 \pm 0.3$ kcal/mol and $D_{0,t} = 1.3 \times 10^{-2 \pm 0.2}$ cm²/s. Similarly, the kinetic parameters for surface diffusion over an isolated step would become $E_s = 5.2 \pm 0.5$ kcal/mol and $D_{0,s} = 3.4 \times 10^{-0 \pm 0.3}$ cm²/s. The close agreement between these kinetic parameters and those given earlier indicates that the error due to minor misalignment of the crystal is minimal.

3. Anisotropy on Ru(001)

The deconvolution analysis assumes that diffusion on the Ru(001) terrace is isotropic. For Ru(001), the surface atoms form a hexagonal array. Because of the surface symmetry, measurement of the terrace diffusion coefficient will not be isotropic for the directions parallel and perpendicular to the step edges.[39] However, the error due to the anisotropy of surface diffusion on the terrace can be evaluated.

n-Butane is thought to diffuse on the terrace through concerted jumps between adjacent groups of threefold sites.[53] For this type of motion, the average distance traveled per jump in the direction perpendicular to the steps is $a_{\perp} = 0.433$ lattice units. In contrast, the average distance traveled in the direction parallel to the steps is $a_{\parallel} = 0.500$ lattice units. Consequently, surface diffusion coefficients in the direction perpendicular to the steps ($D_{\perp}$) should be corrected by dividing by $(a_{\parallel}/a_{\perp})^2 = 0.750$. Because the microscopic diffusion mechanism is not well understood, this correction was not included in the deconvolution analysis. Fortunately, the possible correction is minimal and influences mostly the surface diffusion preexponentials.

4. Value for D_s

The deconvolution analysis assumed that the surface diffusion coefficient over an isolated step D_s is the same in the directions parallel and perpendicular to the step edges. However, steps that may be encountered for molecules diffusing parallel to the step edges are not well defined. Rather than the (100) crystal plane, these steps may expose a different surface plane. The barrier to surface diffusion over the step may depend on the surface plane of the step face. Further studies on other stepped Ru surfaces are needed to address this issue.

5. Value for l_s

The value of $l_s = 4.7$ Å is based on the depiction of the Ru(*S*)-[15(001)×2(100)] surface shown in Fig. 2. This value assumes that a row of atoms from the middle layer of the steps projects out from the step face. If this row of atoms was not present, the step face would be vertical and $l_s = 2.4$ Å.

The surface kinetic parameters for terrace and step diffusion were evaluated using this new value for l_s. The kinetic parameters for the terrace diffusion were identical to those given earlier. Only the preexponential for step diffusion changed in value. The value for $D_{0,s}$ was reduced from $D_{0,s} = 6.1\times10^{-1\pm0.3}$ cm²/s to $D_{0,s} = 3.2\times10^{-1\pm0.3}$ cm²/s. Therefore, the estimation of l_s only affects the preexponential for step diffusion.

C. Effect of steps on Ω

This study of the surface diffusion of *n*-butane on Ru(*S*)-[15(001)×2(100)] indicates clearly that steps influence surface diffusion strongly. However, the measured thermal activation parameters at $\Theta = \Theta_{sat}$ along the terraces of Ru(*S*)-[15(001)×2(100)] are only slightly smaller than the values obtained on Ru(001).[12] The measured corrugation ratio for *n*-butane diffusion on the terraces of Ru(*S*)-[15(001)×2(100)] at $\Theta = \Theta_{sat}$ is $\Omega \equiv E_{dif}/E_{des} = 0.24$. This ratio is 20% lower than the corrugation ratio of $\Omega = 0.29$ for *n*-butane on Ru(001) at $\Theta = \Theta_{sat}$.[18] Given the experimental uncertainties of ± 10%–15% for each value, these corrugation ratios are similar. This similarity indicates that steps are not dominating the LITD measurement of alkane surface diffusion on Ru(001).

The surface diffusion and desorption results for the *n*-alkanes,[12] cycloalkanes,[13] and pentane isomers[14] on Ru(001) explored the effect of molecular chain length, size, and molecular configuration on the diffusion and desorption activation energies. The corrugation ratio was $\Omega \approx 0.3$ for all these alkanes on Ru(001). This nearly constant Ω suggested that the diffusion of all the alkanes on Ru(001) occurred as a result of a concerted molecular motion and that the molecules shared similar binding configurations.

The surface diffusion for *n*-butane on the terraces of Ru(*S*)-[15(001)×2(100)] resulted in a corrugation ratio of $\Omega = 0.24$. In contrast, previous modeling of alkane physisorption on Ru(001) predicted a corrugation ratio of $\Omega \approx 0.10$–0.15.[53] This modeling determined the potential energy surface for alkane adsorption on Ru(001) based on a summation of Lennard-Jones (6-12) pair potentials. One possibility for the discrepancy between theory and experiment was that step defects were dominating the experimental measurements of Ω.

This study of *n*-butane diffusion on Ru(*S*)-[15(001)×2(100)] shows clearly that steps did not dominate the measured corrugation ratios on Ru(001). Given the measured activation barrier for *n*-butane over a step of $E_s = 4.8 \pm 0.5$ kcal/mol, the expected corrugation ratio would be $\Omega = 0.41$ if steps dominated the LITD measurements. Consequently, the discrepancy between the measurements and theory is attributed to modeling alkane adsorption using additive two-body interactions and assuming rigid molecular configurations.[53] A more sophisticated model for surface adsorption and diffusion must be necessary to obtain better agreement with experiment.

The surface diffusion barrier on an isolated terrace of $E_t = 2.8 \pm 0.4$ kcal/mol is lower than the value of $E_{dif} = 3.5 \pm 0.3$ measured previously on Ru(001). The difference is marginally significant within the stated uncertainties of the measurements. This observation suggests that steps may have slightly influenced the previously measured surface diffusion barriers on Ru(001) using LITD methods. However, the activation barriers are close and their similarity argues convincingly that steps did not dominate the LITD measurements.

D. Previous studies

Only a few studies have focused on surface diffusion on stepped surfaces[2–11] and none of these studies have examined the diffusion of physisorbed molecules. The observation that surface steps hinder *n*-butane mobility is consistent with the earlier studies of CO on Pt(111) where steps and defects acted as traps.[9–11] On stepped Pt(111) surfaces, CO diffusion on the Pt(111) terrace was studied with time-resolved infrared spectroscopy. CO bound at a step was far less mobile than CO molecules bound on a terrace.[9,10] Helium scattering techniques have also determined that defects trap CO on Pt(111).[11] However, these studies did not measure CO diffusion over the steps or out of the trap sites.

Several of the previous diffusion studies on stepped surfaces have examined the anisotropy of the diffusion coefficient.[2–6] For adatoms on metal surfaces, an enhancement of the surface diffusion coefficient was observed for diffusion along the step edges.[2–5] In addition, the diffusion barrier over a step was similar to the diffusion barrier on the terrace.[2–6] The enhancement in the surface diffusion coefficient was attributed to an increased concentration of diffusing species at the step edges.[2,3] The increased concentration resulted in a larger concentration gradient and a greater flux of atoms at the step edges compared with the terrace.

Comparisons between physisorbed molecules and chemisorbed atoms are not straightforward because of the vastly different nature of the surface binding. Enhancement of the surface diffusion coefficient may depend on many factors. The main parameters are the fraction of step sites on the surface, the barriers to diffusion along a step and over a terrace, and the difference in binding energy at step and terrace sites.[60] The *n*-butane molecules may be far less mobile in the step sites compared with atomic adsorbates because of the higher adsorption energy and surface corrugation along the step edge.

VI. CONCLUSIONS

The anisotropy of the surface diffusion for *n*-butane on a stepped ruthenium {Ru(*S*)-[15(001)×2(100)]} surface was studied using laser-induced thermal desorption (LITD) methods. A technique was introduced that allowed the components of the diffusion tensor to be measured by utilizing

large aspect ratio desorption areas. Surface diffusion coefficients for diffusion parallel ($D_{\parallel}$) or perpendicular ($D_{\perp}$) to the step edges were measured by orienting these desorption areas with respect to the step edges. The surface diffusion on Ru(S)-[15(001)$\times$2(100)] was clearly anisotropic. At 115 K, the surface diffusion coefficient was larger for diffusion in the direction parallel to the step edges and $D_{\parallel}/D_{\perp} \approx 26$.

Using analogies to heterogeneous diffusion in laminates, the surface diffusion coefficients over a step (D_s) and terrace (D_t) were deconvoluted from $D_{\parallel}$ and $D_{\perp}$. The surface diffusion barrier for *n*-butane diffusion on the terrace was $E_t = 2.8 \pm 0.4$ kcal/mol and the corresponding diffusion preexponential was $D_{0,t} = 1.6 \times 10^{-2 \pm 0.2}$ cm^2/s. These values were slightly smaller than those previously measured on Ru(001). A larger surface diffusion barrier of $E_s = 4.8 \pm 0.5$ kcal/mol and a preexponential of $D_{0,s} = 6.1 \times 10^{-1 \pm 0.3}$ cm^2/s were observed for diffusion over a step. The activation barrier for *n*-butane diffusion over a step was consistent with simple physisorption calculations.

The measured corrugation ratio for *n*-butane diffusion on the terraces of Ru(S)-[15(001)$\times$2(100)] at $\Theta = \Theta_{sat}$ was $\Omega \equiv E_{dif}/E_{des} = 0.24$. This corrugation ratio was slightly smaller than $\Omega = 0.29$ measured previously for *n*-butane on Ru(001). However, the similarity between the corrugation ratios indicated that step defects did not dominate previous LITD measurements of alkanes on Ru(001). Much higher corrugation ratios of $\Omega = 0.41$ would have been measured if steps had governed the diffusion kinetics obtained by LITD techniques.

ACKNOWLEDGMENTS

This work was supported by the National Science Foundation under Grant No. CHE-8908087. Equipment utilized for the computational work was sponsored by NSF under Grant No. CHE-8821737. Some of the equipment used in this work was provided by the NSF-MRL program through the Center for Materials Research at Stanford University. M.V.A. thanks the Eastman Kodak Co. for a graduate fellowship. S.M.G. acknowledges the National Science Foundation for a Presidential Young Investigator Award and the A.P. Sloan Foundation for a Sloan Research Fellowship.

[1] H. Wagner, *Solid Surface Physics* (Springer, New York, 1979).
[2] R. Butz and H. Wagner, Surf. Sci. **87**, 69 (1979).
[3] R. Butz and H. Wagner, Surf. Sci. **87**, 85 (1979).
[4] C. A. Roulet, Surf. Sci. **36**, 295 (1973).
[5] E. Suliga and M. Henzler, J. Phys. C **16**, 1543 (1983).
[6] D. S. Choi, S. Kim, and R. Gomer, Surf. Sci. **234**, 262 (1990).
[7] H. Roux, A. Piquet, R. Uzan, and M. Drechsler, Surf. Sci. **141**, 301 (1984).
[8] T.-S. Lin, H.-J. Lu, and R. Gomer, Surf. Sci. **234**, 251 (1990).
[9] J. E. Reutt-Robey, D. J. Doren, Y. J. Chabal, and S. B. Christman, J. Chem. Phys. **93**, 9113 (1990).
[10] J. E. Reutt-Robey, D. J. Doren, Y. J. Chabal, and S. B. Christman, Phys. Rev. Lett. **61**, 2778 (1988).
[11] B. Poelsema, L. K. Verheij, and G. Comsa, Phys. Rev. Lett. **49**, 1731 (1982).
[12] J. L. Brand, M. V. Arena, A. A. Deckert, and S. M. George, J. Chem. Phys. **92**, 5136 (1990).
[13] C. H. Mak, B. G. Koehler, and S. M. George, J. Vac. Sci. Technol. A **6**, 856 (1988).
[14] M. V. Arena, A. A. Deckert, J. L. Brand, and S. M. George, J. Phys. Chem. **94**, 6792 (1990).
[15] M. V. Arena, E. D. Westre, and S. M. George, J. Phys. Chem. **94**, 4001 (1991).
[16] E. D. Westre, M. V. Arena, A. A. Deckert, J. L. Brand, and S. M. George, Surf. Sci. **233**, 293 (1990).
[17] E. D. Westre, M. V. Arena, and S. M. George (to be published).
[18] M. V. Arena, E. D. Westre, and S. M. George, Surf. Sci. (in press).
[19] J. Crank, *The Mathematics of Diffusion* (Oxford Science, Oxford, 1975).
[20] R. Gomer, Rep. Prog. Phys. **53**, 917 (1990).
[21] C. H. Mak, J. L. Brand, A. A. Deckert, and S. M. George, J. Chem. Phys. **85**, 1676 (1986).
[22] S. M. George, A. M. De Santolo, and R. B. Hall, Surf. Sci. **159**, L425 (1985).
[23] J. P. Cowin, D. J. Auerbach, C. Becker, and L. Warton, Surf. Sci. **78**, 545 (1978).
[24] G. Wedler and H. Ruhmann, Surf. Sci. **121**, 464 (1982).
[25] R. Viswanathan, D. R. Burgess, Jr., P. C. Stair, and E. Weitz, J. Vac. Sci. Technol. **20**, 605 (1982).
[26] B. Roop, S. A. Costello, D. R. Mullins, and J. M. White, J. Chem. Phys. **86**, 3003 (1987).
[27] D. R. Mullins, B. Roop, and J. M. White, Chem. Phys. Lett. **129**, 511 (1986).
[28] E. G. Seebauer, A. C. F. Kong, and L. D. Schmidt, J. Chem Phys. **88**, 6597 (1988).
[29] E. G. Seebauer, A. C. F. Kong, and L. D. Schmidt, J. Vac. Sci. Technol. A **5**, 464 (1987).
[30] C. H. Mak, B. G. Koehler, J. L. Brand, and S. M. George, J. Chem. Phys. **87**, 2340 (1987).
[31] C. H. Mak, B. G. Koehler, J. L. Brand, and S. M. George, Surf. Sci. **191**, 108 (1987).
[32] C. H. Mak, J. L. Brand, B. G. Koehler, and S. M. George, Surf. Sci. **188**, 312 (1987).
[33] J. L. Brand, A. A. Deckert, and S. M. George, Surf. Sci. **194**, 457 (1988).
[34] C. H. Mak, A. A. Deckert, and S. M. George, J. Chem. Phys. **89**, 5242 (1988).
[35] A. A. Deckert, J. L. Brand, M. V. Arena, and S. M. George, Surf. Sci. **208**, 441 (1989).
[36] A. A. Deckert, J. L. Brand, M. V. Arena, and S. M. George, J. Vac. Sci. Technol. A **6**, 794 (1988).
[37] M. Tringides and R. Gomer, J. Chem. Phys. **84**, 4049 (1986).
[38] M. Tringides and R. Gomer, Surf. Sci. **155**, 254 (1985)
[39] D. R. Bowman, R. Gomer, K. Muttalib, and M. Tringides, Surf. Sci. **138**, 581 (1984).
[40] J. L. Brand and S. M. George, Surf. Sci. **167**, 341 (1986).
[41] L. E. Firment and G. A. Somorjai, J. Chem. Phys. **66**, 290 (1977).
[42] L. J. Clarke, *Surface Crystallography* (Wiley, New York, 1985).
[43] M. Henzler, Surf. Sci. **22**, 12 (1970).
[44] B. Lang, R. W. Joyner, and G. A. Somorjai, Surf. Sci. **30**, 440 (1972).
[45] D. W. Blakely and G. A. Somorjai, Surf. Sci. **65**, 419 (1977).
[46] E. D. Williams, W. H. Weinberg, and A. C. Sobrero, J. Phys. Chem. **76**, 1150 (1982).
[47] H. S. Carslaw and J. C. Jaeger, *Conduction of Heat in Solids* (Claredon, Oxford, 1959).
[48] C. H. Mak and S. M. George, Surf. Sci. **172**, 509 (1986).
[49] A. G. Naumovets and Yu. S. Vedula, Surf. Sci. Rep. **4**, 365 (1985).
[50] D. W. Goodman and J. M. White, Surf. Sci. **90**, 201 (1979).
[51] A. A. Deckert, J. L. Brand, C. H. Mak, and S. M. George, J. Chem. Phys. **87**, 1936 (1987).
[52] A. A. Deckert, M. V. Arena, J. L. Brand, and S. M. George, Surf. Sci. **226**, 42 (1990).
[53] M. V. Arena and S. M. George (to be published).
[54] K. J. Laidler, *Chemical Kinetics* (Harper & Row, New York, 1987).
[55] R. J. Behm, W. Hösler, E. Ritter, and G. Binnig, Phys. Rev. Lett. **56**, 228 (1986).
[56] W. J. Kaiser and R. C. Jaklevic, Surf. Sci. **181**, 55 (1987).
[57] W. J. Kaiser and R. C. Jaklevic, Surf. Sci. **182**, L227 (1987).
[58] J. K. Gimzewski, R. Berndt, and R. R. Schlitter, J. Vac. Sci. Technol. B **9**, 897 (1991).
[59] V. M. Hallmark, S. Chiang, and Ch. Wöll, J. Vac. Sci. Technol. B **9**, 1111 (1991).
[60] V. P. Zhdanov, Phys. Lett. A **137**, 409 (1989).